

Simulation and Study of SVPWM Inverter for (VFD) Applications

Ahmed K. Ali and Ergun Ercelebi

Department of Electrical and Electronics Engineering, Gaziantep University, Gaziantep, Turkey

Email: {engineer28ahmed, ergun.ercelebi}@gmail.com

Abstract—Three phase induction motors are representing one of electrical machines is widely used in industrial application, there are many methods to control speed of induction motor. Such as changing the number of stator poles, controlling supply voltage etc. The varying voltage and frequency of three phase supply is a modern method of speed control. In this method can a large amount of energy saving to do so using VFD, the power electronic inverter is a main part of a variable frequency drive. In this paper proposed the simulation of inverter with three types of space vector pulse width modulation SVPWM technique. It is modern and it became a popular PWM for voltage source inverter VSI, the model having advantages for easy control, low cost and achieved to satisfy the requirements of the user. The model is a simulation and analyzed using (SimPower in MATLAB/SIMULINK) environment. The purpose of this paper is to analyze, comparison, and study a three-phase induction motor drive using three types of SVPWM. The simulation results which illustrate the performance of SVPWM system were plotted and discussed. These results are shown variable speed tracking of SGI squirrel cage induction motor, with large scale industrial mechanic load.

Index Terms—SVPWM, SGI, VSI, VFD

I. INTRODUCTION

A DC machine was used for a long time in the industry as a powerful variable speed drive, because of its characteristics like simple controller and fast response. Whereas, AC machines were considered as a constant speed drive when operated at constant voltage and frequency. In the last two or three decades, we have seen extensive research and development efforts for variable speed AC machine drive technology, because of the widely developments in power electronics technology and power semiconductor devices, which lead to replace the major variable speed applications use the DC machine by AC machine drives. This devotion to AC machine comes from the many advantages of AC machines with respect to DC machines. The main advantages of AC machine are, lower cost, light weight (20% to 40% lighter than an equivalent DC machine), easy maintenance compared with DC machine, the squirrel cage type it is lower inertia and losses because it doesn't consist of armature winding and commutator. Have no commutations and brushes problems, which allow a

machine to operate in dirty and moist environments. For these features AC drives are replacing DC drives and they are used in many industrial and domestic applications [1], [2]. A speed control of AC motor important in industrial applications, there are many ways of controlling, a modern and popular one is the constant ratio (V/f), in this method varying the fixed voltage & frequency of three phase supply, to do that, using an inverter with PWM technique. In this paper study SVPWM inverter type, the proposed SVPWM inverter it successfully to change the fixed DC voltage to three phase variable frequency and variable voltage, the synchronous motor speed is given by the equation as [3].

$$N_s = \frac{120f}{p} \quad (1)$$

where, N_s : Synchronous speed (r.p.m), f : Fundamental frequency (Hz), P : Number of poles.

The gap between synchronous speed, and rotor speed, is called the slip.

$$S = \frac{N_s - N_r}{N_s} \quad (2)$$

Also can write

$$N_r = \frac{120f(1 - s)}{p} \quad (3)$$

where N_r : Rotor speed (r.p.m), S : Slip

II. THE MAIN COMPONENTS OF (VFD)

In the variable frequency drive a three phase AC voltage of the supply is rectified into DC, the LC-filter used to reduce ripple, the DC voltage after filtering supply inverter. The six signals of PWM fed the power electronic switches such as (GTO, BJT, IGBT and power MOSFET) [4]. The inverter output feeding induction motor, the basic concept of this process as shown in the following block diagram Fig. 1 and Fig. 2.

A. Full Bridge Rectifier

A full wave three phase bridge rectifier, has six diodes are used to build as shown in Fig. 2a, convert three phase supply (50Hz 480V) or higher, into DC voltage with ripple to limit that ripple used filter [1]

$$V_{Dc} = \frac{3\sqrt{3}V_m}{\pi} \quad (4)$$

Manuscript received January 6, 2016; revised September 14, 2016.

where V_{dc} : Output voltage of rectifier (V), V_m : Peak amplitude of phase voltage of supply (V).

B. DC-Link

The main parts of DC-Link is capacitor and inductors it connected in series between, full bridge rectifier and inverter, as shown in Fig. 2b. [4] The capacitors connected shunt across inverter this topology called a VSI voltage source inverter. The L.C filter in DC -link is designed to provide a limiting a current in DC bus in normal operation of the VFD, also reduced currents harmonic, moreover, improved the power factor across rectifier [5].

C. Inverter

Represent a primary section for VFD, the main part of inverter is power electronic switches, such as (MOSFET or IGBT), the Isolated Gate Bipolar Transistors (IGBT) are very fast electric switches. Can switching by applying small positive voltage across a gate and source, the device will turn ON, also can operate with a high switching frequency (2KHz to 15KHz). The three phase inverter topology shown in Fig. 2c, sometimes called VFD as inverter [3].

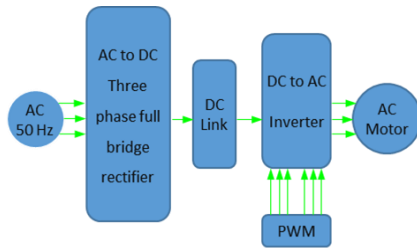


Figure 1. Shows a variable-frequency drive system

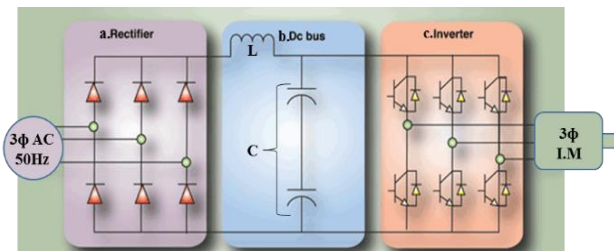


Figure 2. a: Three phase Rectifier circuit, b: DC-link circuit, and c: three phase inverter circuit.

III. CONTROL

The control strategy adjusts the ratio (V/Hz) by using Pulse Width Modulation (PWM) techniques, to produce a varying pulse width, which means that produced varying amplitude in inverter output voltage. The carrier frequency is represented a speed of turning (ON and OFF) switches, it is noted that the carrier frequency increase leads to get more sinusoidal in inverter output waveform. [6] To maintain the (V/f) ratio is constant, so as lead to stator magnetic flux remain constant, if varying only the frequency and same voltage is applied to AC machine, that caused an increase in stator magnetic flux till to the saturation magnetic core, this lead to a low performance of motor [4].

$$V_{Ph} = 4.44kfN\phi_m \quad (5)$$

$$\frac{V_{Ph}}{f} = 4.44kN\phi_m \quad (6)$$

And:

$$T = k \cdot \phi_m \cdot I_2 \quad (7)$$

where ϕ_m : Magnetizing flux (W.b), N : Number of turns per phase. V_{Ph} : Stator voltage (V). K : Constants depend on the Machine design, T : Shaft torque (N.M), I_2 : Rotor current (A) depends on the load [5].

To avoid saturation in stator magnetic core, keeping the (V/f) ratio constant, to maintaining motor torque constant at all speed below the rated speed must be remain the flux is a constant value from (7), which is keeping the (V/f) ratio constant. If reduce the motor speed to 50%, the voltage reduced to (V/2) and frequency (f/2), that keeping a stator flux constant, which is given constant output torque [7], [8].

There are four basic types of control for AC drive:

- 1) Volt-per-hertz it is a scalar control method, providing variable speed by keeping (V/f) ratio constant. This type of control used for application, such as fan and pump, it provides constant torque with fair speed, represents a low cost method.
- 2) Sensor less vector this method of control produce, high starting torque with batter speed.
- 3) Flux vector control, this method of control provides high accuracy speed and torque by using closed loop feedback.
- 4) Fielded oriented control, this method proved more control to the AC motor perimeter, such as speed and torque, it gives the best performance of AC motor equal, to the DC motor.

IV. SPACE VECTOR PULSE WIDTH MODULATION TECHNIQUE FOR VSI

A. Voltage Source Inverter (VSI)

A voltage source inverter VSI must have a stiff voltage source at the input that is Thevenin impedance must be ideally equal to zero. Thus is can be represented a large capacitor connected at the input, if the voltage source is not stiff. The Fig. 3, shows a practical VSI consist of power bridge devices with three output legs [9], each consisting of two power electronic switches each of the switches has freewheeling diodes, and the inverter is supplied from a DC source (either battery or diode-based bridge rectifier via C or L.C filter) [5].

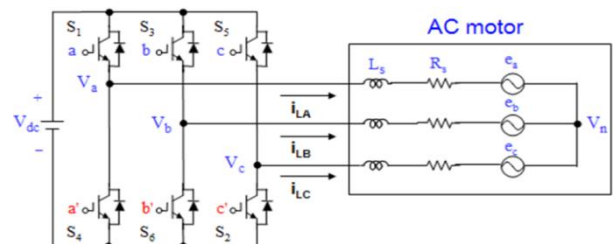


Figure 3. Voltage Source Inverter (VSI) topology.

In VSI always the semiconductor switches, remain forward biased due to the DC supply voltage, therefore, self-controlled forward or asymmetric blocking devices, [2], are suitable for inverter such as, (GTOs, BJTs, IGBTs and power MOSFETs). One important characteristic of the VSI, is that the inverted AC voltage wave is not affected by the load parameters [3].

B. Principle of SVPWM

A digital SVPWM are becoming popular in PWM inverter, the traditional triangular carrier method has been overcome, by the SVPWM. Because of its high performance characteristics in inverter applications, it has found widespread applications in recent years. With a pulse width modulation PWM. [10] The inverter can thought as three separate push-pull drive stages, which create each phase waveform independently. However, SVPWM treats the inverter as a single unit with a machine mechanic load, the machine load neutral is normally isolated [11], which causes interaction among the phases. This interaction was not considered before in PWM. The space vector PWM method considers this interaction of the phases and optimizes, the harmonics of 3-phase isolated neutral load. [1]

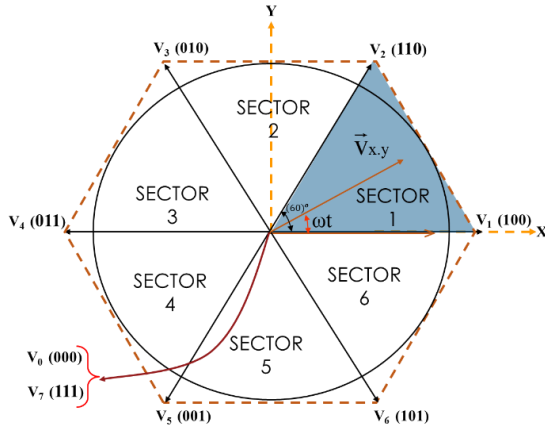


Figure 4. Hexagon boundary with six sectors.

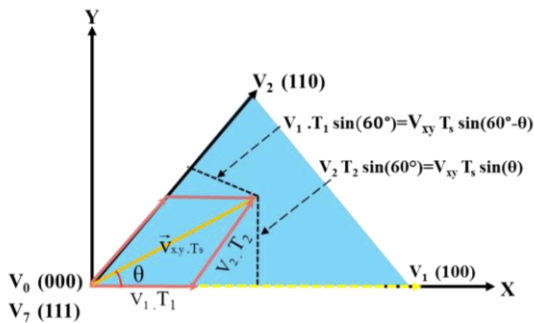


Figure 5. Reference vector at sector 1.

In SVPWM technique, the three phases (A, B, C) coordinate system are transferred to two frames axis (X, Y), [9] which are a complex axis frame the (X-axis) represents a real axis, and (Y-axis) represents a direct imaginary axis. The “ V_{xy} ” is referring to voltage vector, this vector rotating at a constant angular frequency (ω), in SVPWM ($V_1, V_2, V_3, V_4, V_5, V_6$) represent vectors in plan,

this plan divide into six sectors, each sector, having ($\pi/3$) or (60°), as shown in Fig. 4, a reference voltage “ V_{xy} ” is synthesized by adjacent two nulls zero vector (V_1 to V_6), and two zero vector (V_0 & V_7), as shown in Fig. 5. The radius of inside circle is ($\frac{1}{\sqrt{3}} V_{DC}$). The outputs three phase sinusoidal voltage cycle is rising when reference voltage is revolving in space, the cycle is completed during one revolution of (V_{xy}) [3].

Generally, each sector of the hexagon is divided into (sub-sectors), in which the reference voltage “ V_{xy} ” will move in angular steps ($\omega.t$), the width of the steps (sub-sector angle), depends on the maximum permissible switching rate of the power electronic devices, whenever step width is small and switching frequency is high, the output fundamental voltage will be close to sinusoidal [9].

V. IMPLEMENTATION OF (SVPWM)

There are two methods can be implemented the SVPWM [12]. The first by sector selection based on modulation the second by SVPWM based on the carrier frequency. In this paper implemented these types:

- SVPWM based on the sector selection.
- SVPWM without sector, based on the carrier frequency.
- SVPWM based on the carrier frequency with reduced switching.

A. Implementation of SVPWM with Sector Selection

This method can be summarized by the following steps

Step A: Determine (V_x, V_y, V_{xy}) and angle (θ)

Step B: Determine time duration (T_1, T_2, T_0)

Step C: Determine the switching time of each power transistor (S_1 , to S_6).

Step A: Determine (V_x, V_y, V_{xy}) and angle (θ): to understand the theory of SVPWM [9], the idea of a rotating space vector and, axis transformation is very important. Any three quantities can be expression by two axis frames (V_x, V_y). [9], [10], [13], [14] the transformation procedure can easily done by the following formula [3].

$$\begin{bmatrix} V_x \\ V_y \end{bmatrix} = \frac{2}{3} \begin{bmatrix} \cos(0) & \cos(120^\circ) & \cos(-120^\circ) \\ \sin(0) & \sin(120^\circ) & \sin(-120^\circ) \end{bmatrix} \begin{bmatrix} V_a \\ V_b \\ V_c \end{bmatrix} \quad (8)$$

$$\text{or } \begin{bmatrix} V_x \\ V_y \end{bmatrix} = \frac{2}{3} \begin{bmatrix} 1 & -1/2 & -1/2 \\ 0 & \sqrt{3}/2 & -\sqrt{3}/2 \end{bmatrix} \begin{bmatrix} V_a \\ V_b \\ V_c \end{bmatrix} \quad (9)$$

The result of the matrix is given:

$$V_x = \frac{2}{3} (V_a - \frac{1}{2}V_b - \frac{1}{2}V_c) \quad (10)$$

$$V_y = \frac{2}{3} ((0)V_a + \frac{\sqrt{3}}{2}V_b - \frac{\sqrt{3}}{2}V_c) \quad (11)$$

When:

$$V_{xy} = V_x + jV_y \quad (12)$$

$$\begin{aligned} V_{xy} &= \frac{2}{3} \left[\left(V_a - \frac{1}{2}V_b - \frac{1}{2}V_c \right) + j \left(\frac{\sqrt{3}}{2}V_b - \frac{\sqrt{3}}{2}V_c \right) \right] \\ &= \frac{2}{3} \left[V_a + \left(-\frac{1}{2} + j\frac{\sqrt{3}}{2} \right) V_b + \left(-\frac{1}{2} - j\frac{\sqrt{3}}{2} \right) V_c \right] \\ V_{xy} &= \frac{2}{3} [V_a + aV_b + a^2V_c] \quad (13) \end{aligned}$$

where:

$$a = -\frac{1}{2} + j\frac{\sqrt{3}}{2} = e^{j\frac{2\pi}{3}}, \text{ and } a^2 = -\frac{1}{2} - j\frac{\sqrt{3}}{2} = e^{-j\frac{2\pi}{3}}$$

To find (θ) from (12):

$$V_{xy} = \sqrt{(V_x)^2 + (V_y)^2} \quad (14)$$

$$\theta = \tan^{-1}\left(\frac{V_y}{V_x}\right) \quad (15)$$

$$\theta = 2\pi f_s t$$

Step B: Determine time duration (T_1, T_2, T_0) : The space reference voltage “ V_{xy} ”, moves from state-1 to state-2 by time sharing PWM between $(V_1 \& V_2)$ [3], [13], for example in Fig. 5 if the vector “ V_{xy} ” Lies in sector-1 the PWM adjusted between V_1 (100) and V_2 (110) by the duty cycle of each $(T_1 \& T_2)$, is respectively the zeroes vectors $(V_0$ (000) & V_7 (111)) of duty cycle (T_0) [1].

The volt-second duration at Sector1 is:

$$\int_0^{T_s} V_{xy} dt = \int_0^{T_1} V_1 dt + \int_{T_1}^{T_1+T_2} V_2 dt + \int_{T_1+T_2}^{T_0} (V_0 \text{ or } V_7) dt$$

$$T_s V_{xy} = T_1 V_1 + T_2 V_2 + T_0 (V_0 \text{ or } V_7) \quad (16)$$

where: $(V_0 \text{ or } V_7) = 0V$ at output of the inverter.

$$V_{xy} = \frac{T_1}{T_s} V_1 + \frac{T_2}{T_s} V_2 + (V_0 \text{ or } V_7) \frac{T_0}{T_s} \quad (17)$$

Also from Fig. 5, can be found (V_{an}, V_{bn}) , of sector one.

$$V_{xy} \cdot T_s \sin\left(\frac{2\pi}{6} - \theta\right) = V_1 \cdot T_1 \sin\left(\frac{2\pi}{6}\right)$$

and

$$V_{xy} \cdot T_s \sin(\theta) = V_2 \cdot T_2 \sin\left(\frac{2\pi}{6}\right)$$

where $(V_{xy} = V_{an} + V_{bn})$, and from (17):

$$V_{an} = \frac{T_1}{T_s} V_1 \quad V_{bn} = \frac{T_2}{T_s} V_2$$

$$\Rightarrow V_{an} = \frac{2}{\sqrt{3}} V_{xy} \sin\left(\frac{2\pi}{6} - \theta\right)$$

$$V_{bn} = \frac{2}{\sqrt{3}} V_{xy} \sin(\theta)$$

If:

$$V_n(u) = \frac{2}{3} V_{DC} e^{j(u-1)\frac{\pi}{3}}$$

where $(u: 1, 2, 3...6)$ the phase voltages space vectors $V_1(100) = \frac{2V_{DC}}{3}$, and after “ 60° ” $V_2(110) = \frac{2V_{DC}}{3}$.

That leads to:

$$T_1 = \sqrt{3} \frac{V_{xy}}{V_{DC}} T_s \sin\left(\frac{2\pi}{6} - \theta\right) \quad (18)$$

$$T_2 = \sqrt{3} \frac{V_{xy}}{V_{DC}} T_s \sin(\theta) \quad (19)$$

$$T_0 = T_s - T_1 - T_2 \quad (20)$$

$$T_s = \frac{1}{f_s}$$

where (T_s) , is the sampling time period of the switching frequency (f_s) , and (V_{DC}) DC link voltage. The modulation index is:

$$m_i = \frac{\sqrt{3} V_{xy}}{V_{DC}}$$

The time interval $(T_1 \text{ and } T_2)$, satisfies the reference voltage, but (T_0) , fill up the remaining gap in (T_s) , as shown in Fig. 6, Fig. 7, and Fig. 8 [1].

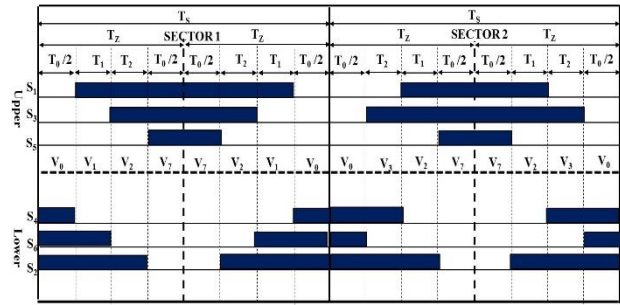


Figure 6. Switching time of $(S_1 \text{ to } S_6)$ at Sector (1, 2).

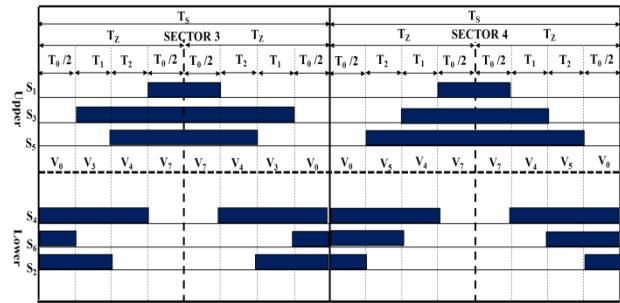


Figure 7. Switching time of $(S_1 \text{ to } S_6)$ at Sector (3, 4).

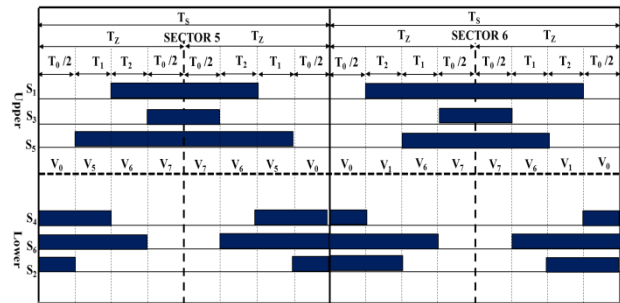


Figure 8. Switching time of $(S_1 \text{ to } S_6)$ at Sector (5, 6).

The Switching time duration at any sector in the hexagon.

$$T_1 = \sqrt{3} \frac{V_{xy}}{V_{DC}} T_s \sin\left(\frac{2\pi}{6} - \theta + \frac{(n-1)\pi}{3}\right) \quad (21)$$

$$T_2 = \sqrt{3} \frac{V_{xy}}{V_{DC}} T_s \sin\left(\theta - \frac{(n-1)\pi}{3}\right) \quad (22)$$

$$0 \leq \theta \leq 60$$

where (n) is the number of sectors (1 to 6), and (θ) sub-sector angle.

Step C: Determine the switching time of each switching device (S_1 to S_6): The switching sequence pattern for each power electronic switch device, as shown in Fig. 6, Fig. 7 and Fig. 8. Table I is summarizing the switching time for each sector [9].

$$T_z = \frac{T_s}{2}$$

TABLE I. SWITCHING TIME FOR EACH SECTOR

Sectors (n)	Upper switching (S_1, S_3, S_5)	Lower switching (S_4, S_6, S_2)
1	$S_1 = T_1 + T_2 + \frac{T_0}{2}$ $S_3 = T_2 + \frac{T_0}{2}$ $S_5 = \frac{T_0}{2}$	$S_4 = \frac{T_0}{2}$ $S_6 = T_1 + \frac{T_0}{2}$ $S_2 = T_1 + T_2 + \frac{T_0}{2}$
2	$S_1 = T_1 + \frac{T_0}{2}$ $S_3 = T_1 + T_2 + \frac{T_0}{2}$ $S_5 = \frac{T_0}{2}$	$S_4 = T_2 + \frac{T_0}{2}$ $S_6 = \frac{T_0}{2}$ $S_2 = T_1 + T_2 + \frac{T_0}{2}$
3	$S_1 = \frac{T_0}{2}$ $S_3 = T_1 + T_2 + \frac{T_0}{2}$ $S_5 = T_2 + \frac{T_0}{2}$	$S_4 = T_1 + T_2 + \frac{T_0}{2}$ $S_6 = \frac{T_0}{2}$ $S_2 = T_1 + \frac{T_0}{2}$
4	$S_1 = \frac{T_0}{2}$ $S_3 = T_1 + \frac{T_0}{2}$ $S_5 = T_1 + T_2 + \frac{T_0}{2}$	$S_4 = T_1 + T_2 + \frac{T_0}{2}$ $S_6 = T_2 + \frac{T_0}{2}$ $S_2 = \frac{T_0}{2}$
5	$S_1 = T_2 + \frac{T_0}{2}$ $S_3 = \frac{T_0}{2}$ $S_5 = T_1 + T_2 + \frac{T_0}{2}$	$S_4 = T_1 + \frac{T_0}{2}$ $S_6 = T_1 + T_2 + \frac{T_0}{2}$ $S_2 = \frac{T_0}{2}$
6	$S_1 = T_1 + T_2 + \frac{T_0}{2}$ $S_3 = \frac{T_0}{2}$ $S_5 = T_1 + \frac{T_0}{2}$	$S_4 = \frac{T_0}{2}$ $S_6 = T_1 + T_2 + \frac{T_0}{2}$ $S_2 = T_2 + \frac{T_0}{2}$

B. SVPWM Based on the Carrier

The carrier based on SVPWM is efficient, fast, and easier implementation, this technique is based on comparing the duty cycle ratio as shown in Fig. 9, with the triangular waveform, a triangular waveform frequency is (f_s), it can be set by the user [12], the digital pulses are arranged as same as sinusoidal pulse width modulation [15].

C. SVPWM Based on a Carrier with Reduce d Switching

The SVPWM based on a carrier with reduced switching ratio, is the better implementation of SVPWM because, the switching ratio can be reduced to 33%, that leads to reduce the heat of switches, the method based on choosing one side either mini or max from three control signals [12], as shown in Fig. 10

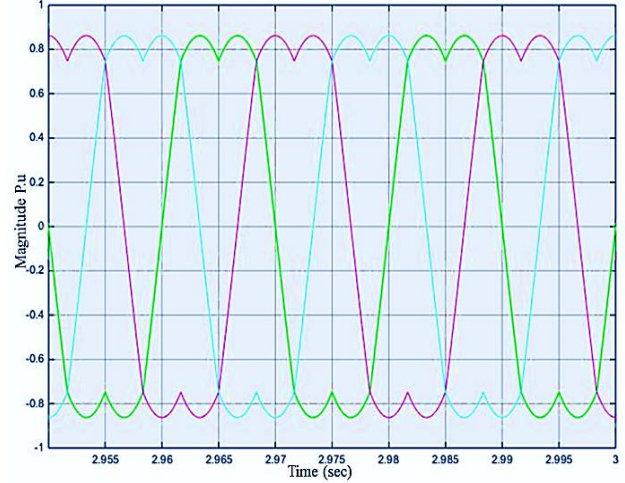


Figure 9. Duty cycle ratio of SVPWM based on the carrier.

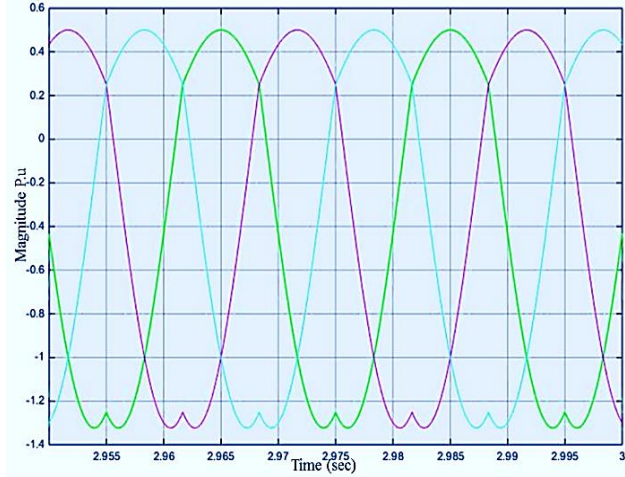


Figure 10. Duty cycle ratio of SVPWM based on a carrier with reduced switching.

VI. SIMULAT THE (SVPWM) USING MATLAB

A. (SVPWM) with Sector Selection

The SIMLINK block in the Fig. 11 shows calculate (V_{xy}) & (θ), in Fig. 12 are shown MATLAB SIMLINK block to generate six sectors, the (T_1 , T_2 & $T_0/2$) is implementation form equations ((20), (21), (22)), by using S-function as shown in Fig. 13. From Table I, and compared with high frequency triangular waveform, that can be generated transistor switching signal (S_1 to S_6), Fig. 14 illustrates this process. The MATLAB subsystem blocks of the SVPWM based on sector selection are shown in Fig. 15.

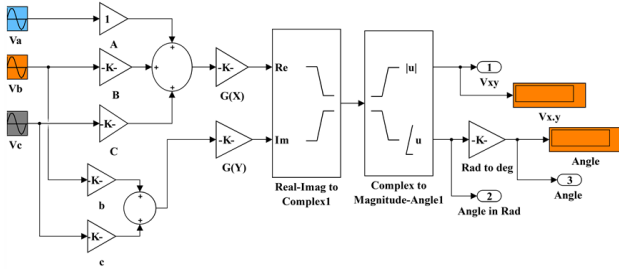


Figure 11. Illustrates of implementation of (V_{xy}) and angle (θ).

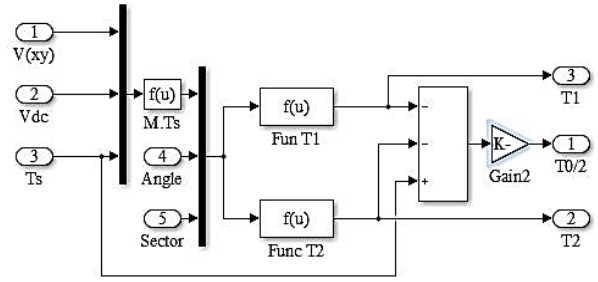


Figure 13. Implementation the (T_1 , T_2 & $T_0/2$)

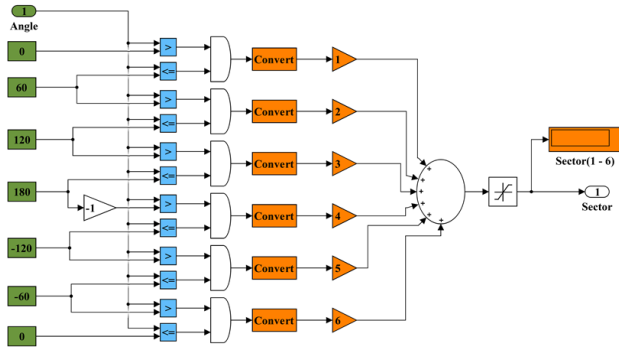


Figure 12. Blocks to generate six sectors (1 to 6).

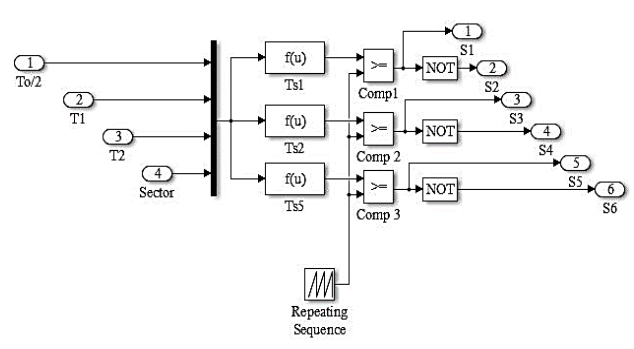


Figure 14. Implementation the transistor switching signal (S_1 to S_6).

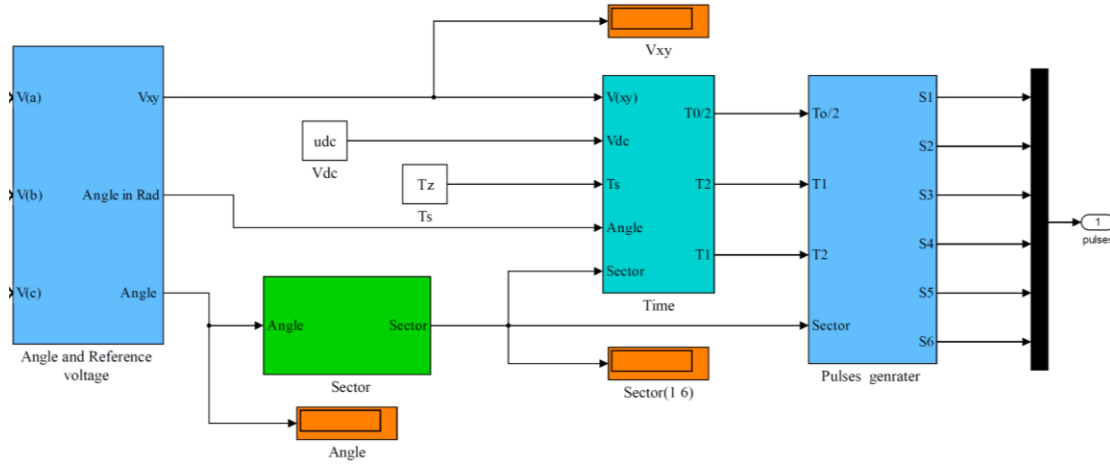


Figure 15. Blocks model to the SVPWM based on the sector selection technique.

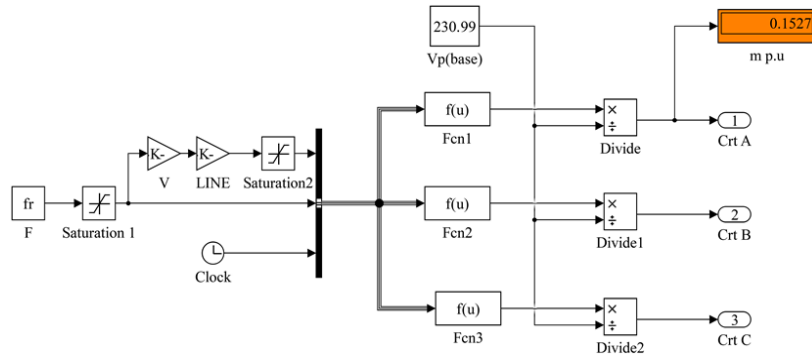


Figure 16. MATLAB/ SIMULINK blocks shown, how can calculate (V/f) ratio.

B. Implementation of (SVPWM) Based on Carrier, and SVPWM Reduced Switching

The implementation are summered briefly by this step
1) Generate three sinusoidal waveforms as shown in Fig. 16.

- 2) Using a mini-max MATLAB block to find the highest value and the lowest value from the three signals in the Fig. 16.
- 3) Add the maximum signal to the minimum and the output is multiplied by 0.5 to reduce a magnitude.

- 4) Subtract the output from step (3), from three sinusoidal waveforms in the step (1) as shown in Fig. 17.
- 5) Comparing the output from step (4), with the triangle waveform, (magnitude=1 and carrier frequency f_s). The overall (MATLAB/SIMULINK) scheme of SVPWM based on carrier as shown in Fig. 17, and the scheme of SVPWM with reduced switching as shown in Fig. 18.

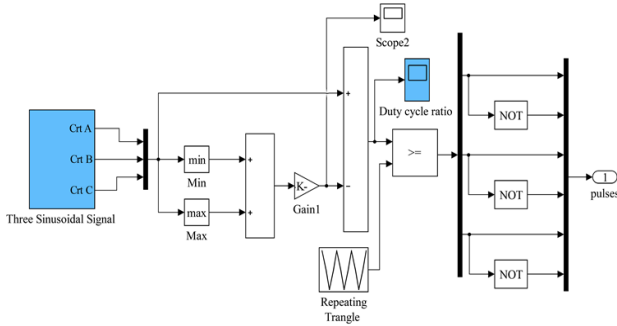


Figure 17. MATLAB/SIMULINK scheme of SVPWM based on the carrier.

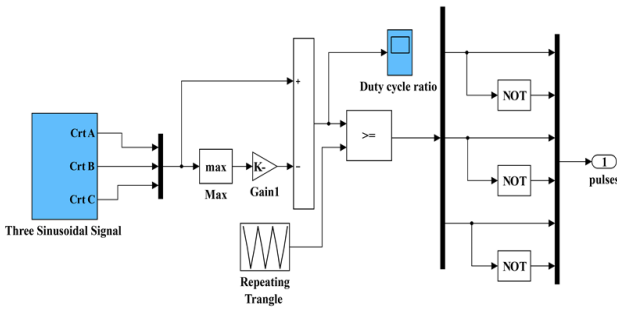


Figure 18. MATLAB/SIMULINK scheme of SVPWM based on a carrier with reduced switching ratio.

VII. (MATLAB/SIMULINK) ANALYSIS OF SVPWM INVERTER BASED ON (VFD)

A. Design Values for Proposed VFD MATLAB Model

- Types of simulation: Discrete backward Euler, sample time (10 μ s).
- Rectifier and DC link filter: in this paper we will, assume, the three phase rectifier, and filter is a constant DC source (DC-Link voltage = 630V), as shown in Fig. 19.
- SVPWM specification: switching frequency f_s : 8KHz, rated frequency, f_r : 50Hz.
- Inverter: Universal Bridge block in the (MATLAB/SIMULINK). The inverter specification are listed in the Table A.1 in the Appendix (A).

B. Asynchronous Machine Specification

Squirrel cage Induction motor, the motor parameters and specification are listed in the Table A.2, in the Appendix (A).

C. Load Specification

The mechanical load is assuming large scale industrial fan, which is shown in Fig. 20, the model is built using the equations in (MATLAB/ SIMULINK).

$$T_l = K (\omega)^2 \quad (23)$$

$$T = \frac{P_o}{\omega}$$

$$\omega_r = \frac{2\pi(1430)}{60} = \frac{143}{3} \pi \text{ red/Sec} \quad (24)$$

$$T_m = \frac{5.4 \times 746}{149.749} = 26.9 \approx 27 \quad (25)$$

From (23)

$$K = \frac{27}{(149.749)^2} \approx 1.20 \times 10^{-3} \quad (26)$$

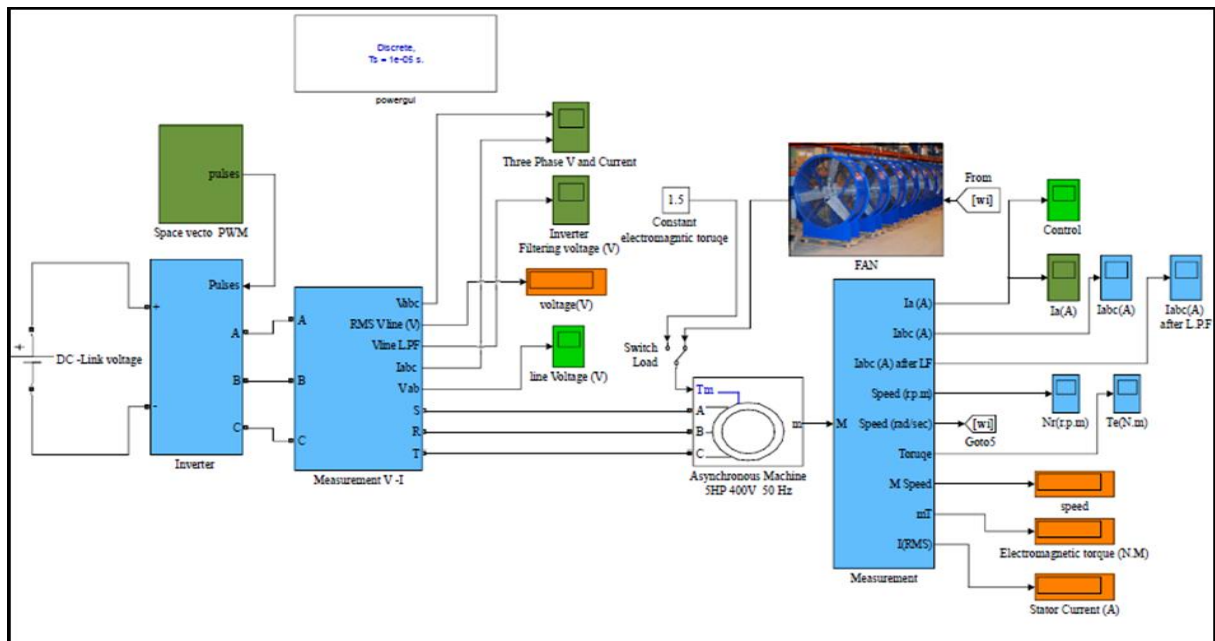


Figure 19. Subsystem block diagram of (VFD) based SVPWM inverter, feeding three phase squirrel cage induction motor.

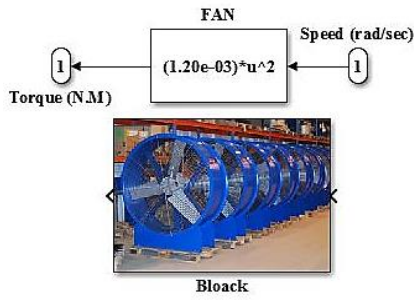


Figure 20. Illustration of large scale industrial fan.

Calculated the ratio (V/f): The asynchronous machine rated line to line voltage is: (400V), and phase voltage: (230.94V), or (0.995) P.u if the base voltage (230.99V), the frequency given a base speed (1430 r.p.m), is (50Hz), the ratio ($K_r=4.6$). The MATLAB blocks and using S-functions to implanted three sinusoidal control signals (Crt_A , Crt_B , Crt_C), with varying magnitude (46 to 230) V, or (0.19 to 0.995) P.u. The variability in the magnitude depends on this ratio ($4.6*f_r$), in the Fig. 16 shows generate three signals with varying magnitude. The function of the saturation (1) in the Fig. 16, is determining minimum and maximum of the rated frequency ($f_{r\text{ Mini}}$, $f_{r\text{ Max}}$), and the saturation (2) it used to determine a minimum and maximum magnitude ($V_{r\text{ Mini}}$, $V_{r\text{ Max}}$), also this parameter can be set by the user, the (V/f) calculated scheme having one variable at input, and three signals in output side, the (f_r) referred to user required frequency. The three phase sinusoidal waveforms [16].

$$Crt_A = V \sin(2\pi f_r t)$$

$$Crt_B = V \sin(2\pi f_r t + 2\pi/3)$$

$$Crt_C = V \sin(2\pi f_r t - 2\pi/3)$$

where $t=10$ Sec

$$K_r = \frac{230.94}{50} = 4.6 \quad (27)$$

VIII. SIMULATION RESULTS

The simulation results will consist of two parts. The first part will show the System performance without any change in frequency. The second part will show the System performance after frequency variation with different value. The parameters of the induction motor are listed in Table A.2, in the Appendix (A). Fig. 21(a, b, c) shows the Total harmonic distortion in the stator current waveform in three types of SVPWM at no load, in Fig. 22 (a, b, c), the THD of the stator current when the machine running under load conditions, and the THD for line voltage in three types of SVPWM are shown in Fig. 23(a, b, c). The THD for voltage & current under two conditions are listed in Table II. The stator current when using three types of SVPWM is shown in Fig. 24 (a, b, c) & Fig. 25 (a, b, c). The line voltage for three types of SVPWM after 2-order low pass filter having cut off frequency ($4*f_r$), are shown in Fig. 26 (a, b, c). The electromagnetic torque (N.M), and rotor speed (r.p.m) is shown respectively in Fig. 27(a, b, c) and Fig. 28 (a, b, c),

under operating system at rated frequency with a large industrial fan attached to the motor. Table III and Table IV will show the System performance after variation frequency, the line voltage, and rotor speed is listed.

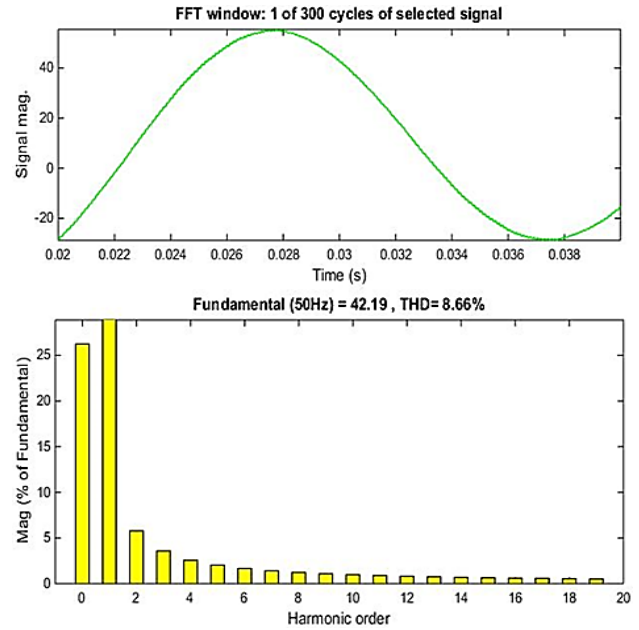


Figure 21a. THD (%) of current waveform at no load for SVPWM based on the sector at $f_r=50$ Hz.

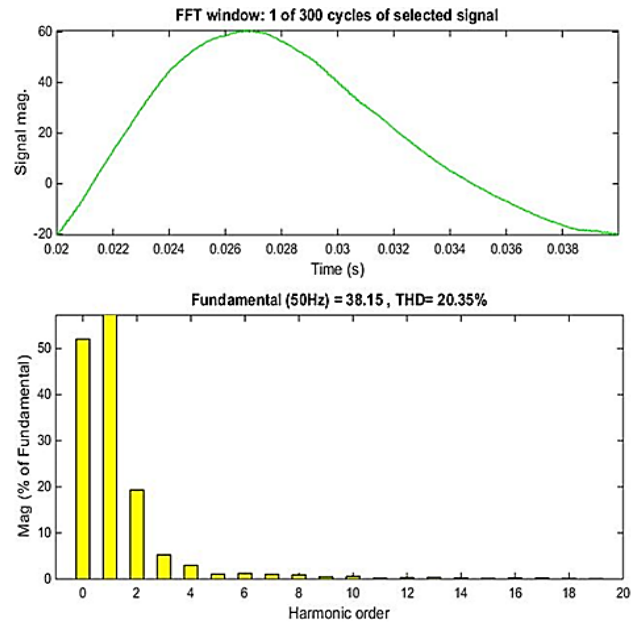
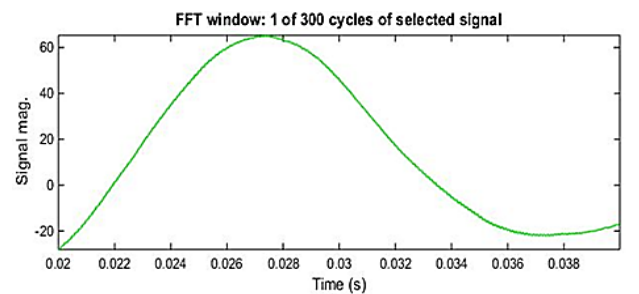


Figure 21b. THD (%) of current waveform at no load for SVPWM based on the carrier frequency at $f_r=50$ Hz.



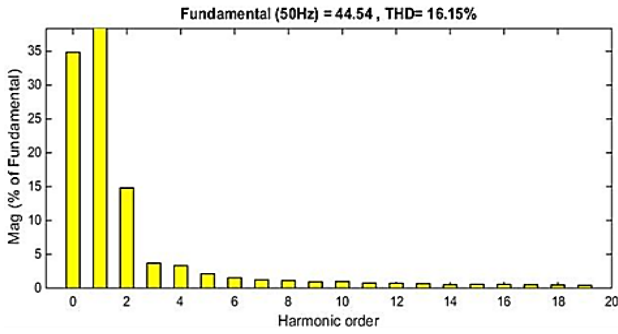


Figure 21c. THD (%) of current waveform at no load for SVPWM based on the carrier frequency with reduced switching at $f_r=50\text{Hz}$.

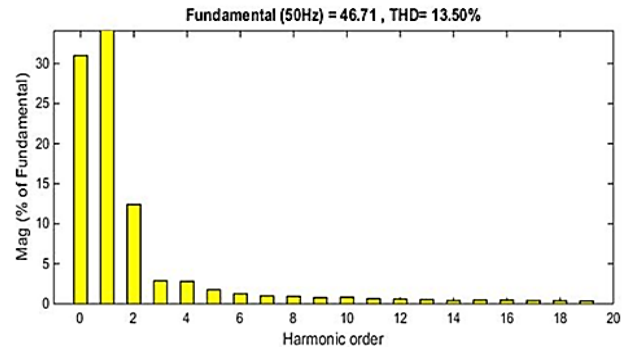
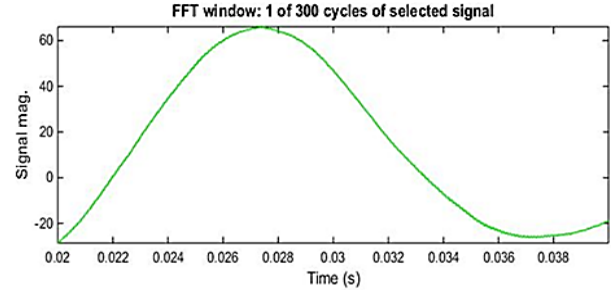
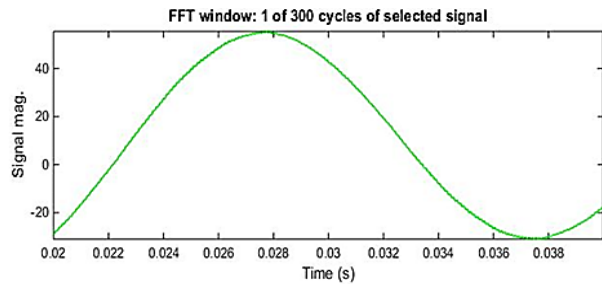


Figure 22c. THD (%) of current waveform at load condition for SVPWM based on the carrier frequency with reduced switching at $f_r=50\text{Hz}$.

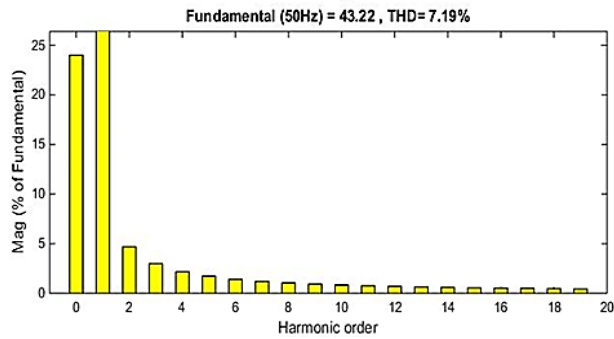


Figure 22a. THD (%) of current waveform at load condition for SVPWM based on the sector at $f_r=50\text{Hz}$.

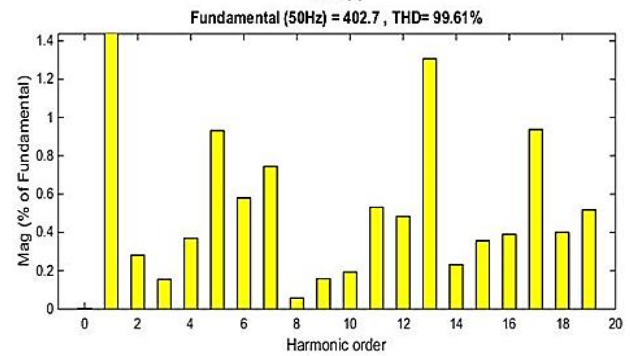
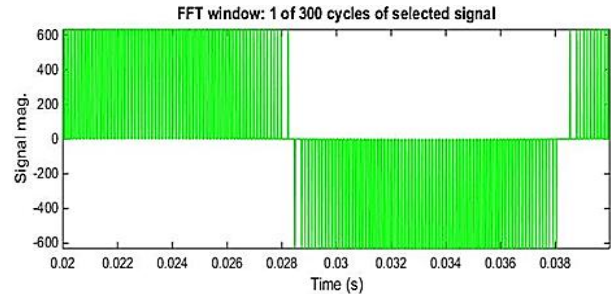
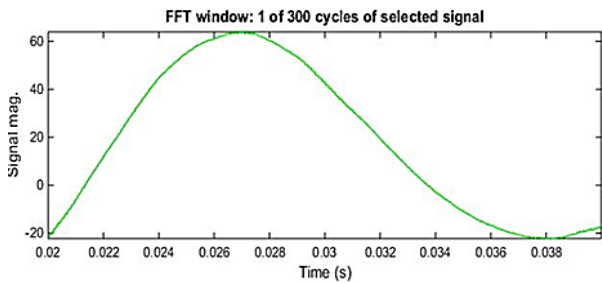


Figure 23a. THD (%) of the line voltage waveform for SVPWM based on the sector at $f_r=50\text{Hz}$.

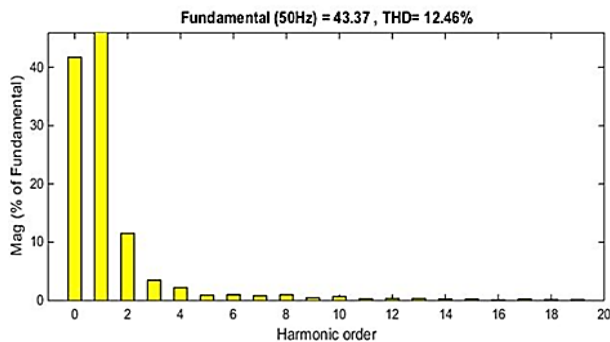
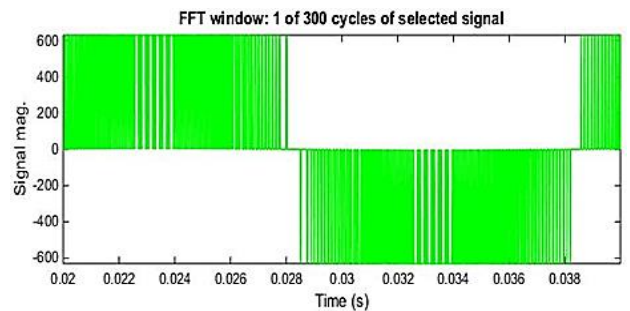


Figure 22b. THD (%) of current waveform at load condition for SVPWM based on the carrier frequency at $f_r=50\text{Hz}$.



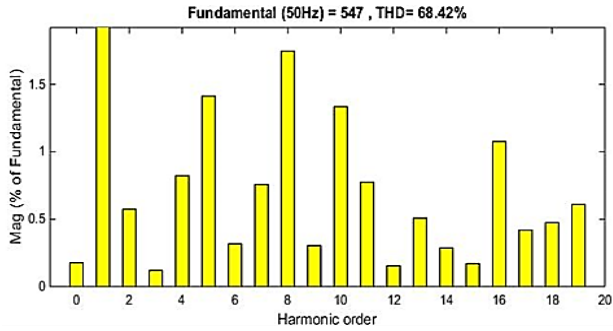


Figure 23b. THD (%) of the line voltage waveform for SVPWM based on the carrier frequency at $f_r=50\text{Hz}$.

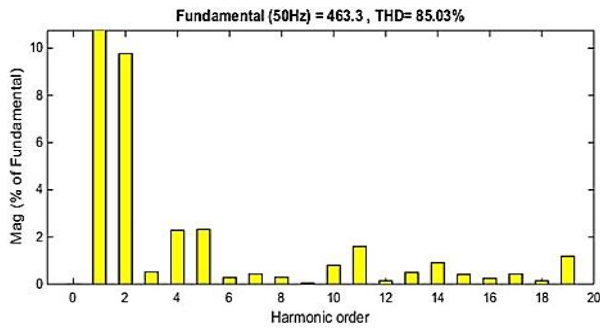
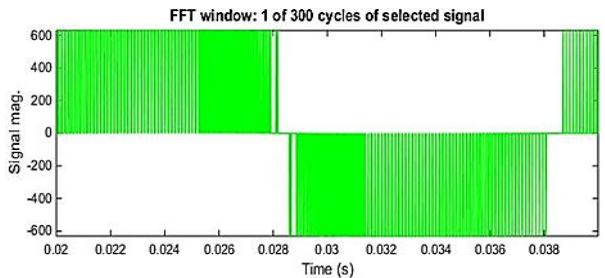


Figure 23c. THD (%) of the line voltage waveform for SVPWM based on the carrier frequency with reduced switching at $f_r=50\text{Hz}$.

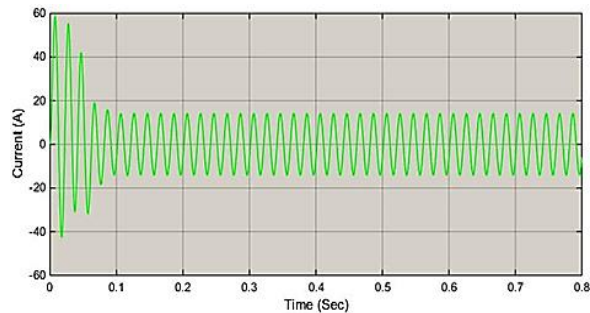


Figure 24a. Stator current (A) for SVPWM based on the sector at $f_r=50\text{Hz}$.

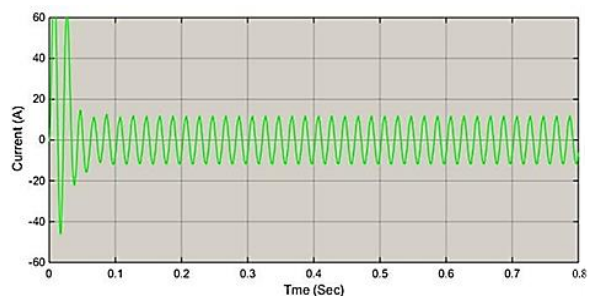


Figure 24b. Stator current (A) for SVPWM based on the carrier frequency at $f_r=50\text{Hz}$.

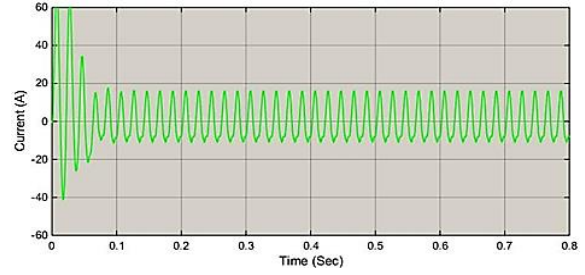


Figure 24c. Stator current (A) for SVPWM based on the carrier frequency with reduced switching at $f_r=50\text{Hz}$.

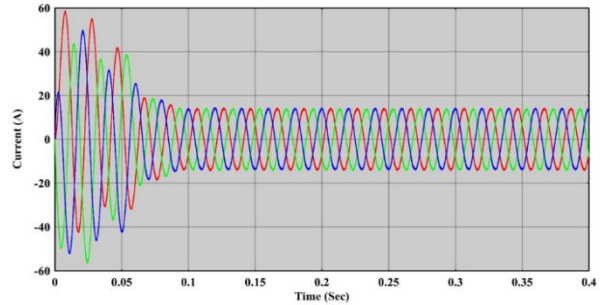


Figure 25a. Three phase current (A) for SVPWM based on the sector at $f_r=50\text{Hz}$.

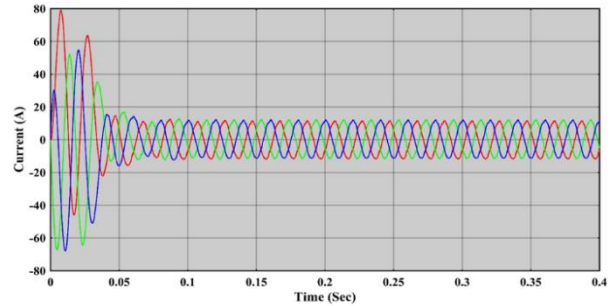


Figure 25b. Three phase current (A) for SVPWM based on the carrier frequency at $f_r=50\text{Hz}$.

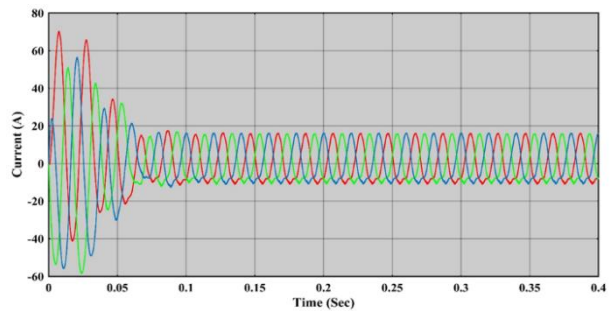


Figure 25c. Three phase current (A) for SVPWM based on the carrier frequency with reduced switching at $f_r=50\text{Hz}$.

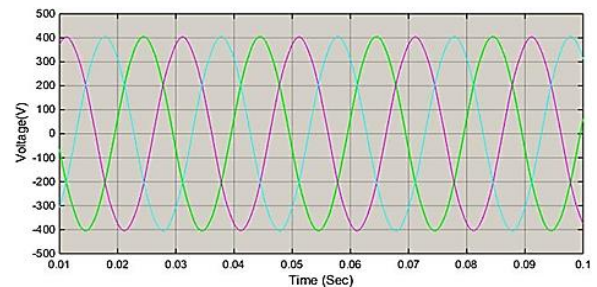


Figure 26a. Three phase line voltage (V) for SVPWM based on the sector after (2nd-order low pass filter) at $f_r=50\text{Hz}$.

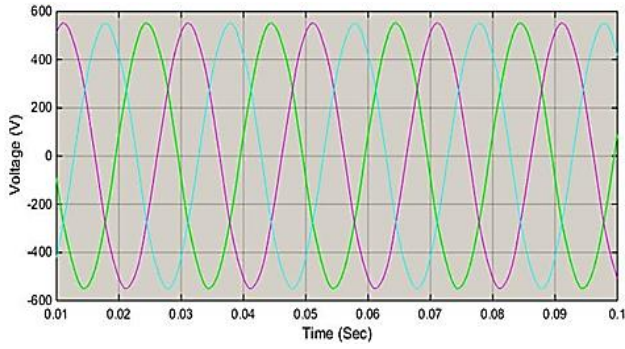


Figure 26b. Three phase line voltage (V) for SVPWM based on the carrier frequency after (2nd-order low pass filter) at $f_r=50\text{Hz}$.

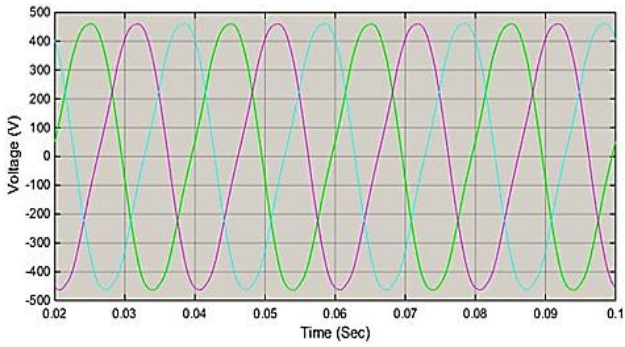


Figure 26c. Three phase line voltage (V) for SVPWM based on the carrier frequency with reduced switching after (2nd-order low pass filter) at $f_r=50\text{Hz}$.

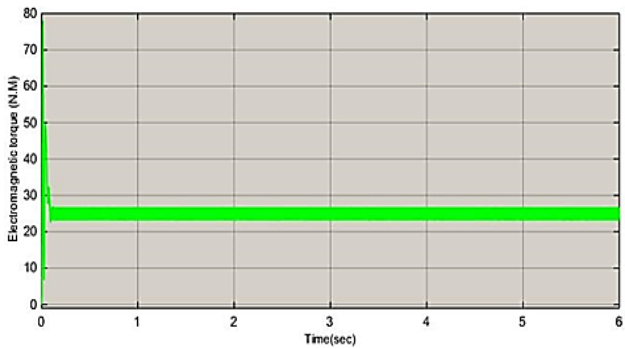


Figure 27a. Electromagnetic torque (N.M) under load condition for SVPWM based on the sector at $f_r=50\text{Hz}$.

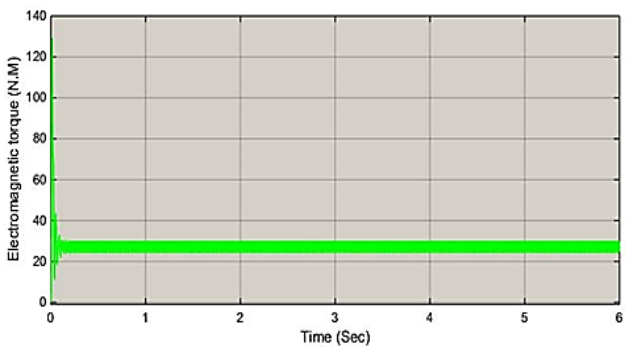


Figure 27b. Electromagnetic torque (N.M) under load condition for SVPWM based on the carrier frequency at $f_r=50\text{Hz}$.

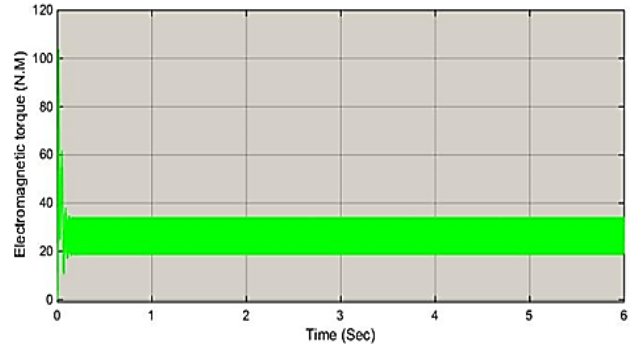


Figure 27c. Electromagnetic torque (N.M) under load condition SVPWM based on the carrier frequency with reduced switching at $f_r=50\text{Hz}$.

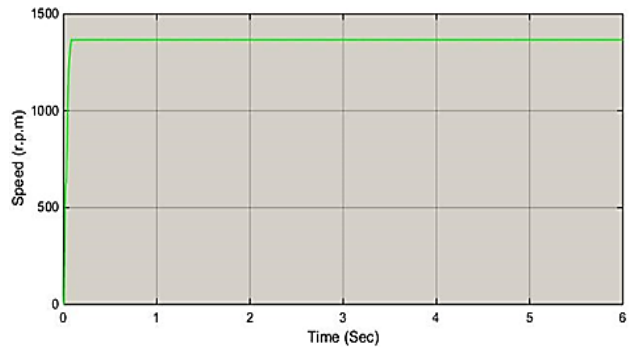


Figure 28a. The rotor speed (r.p.m) for SVPWM based on the sector at $f_r=50\text{Hz}$.

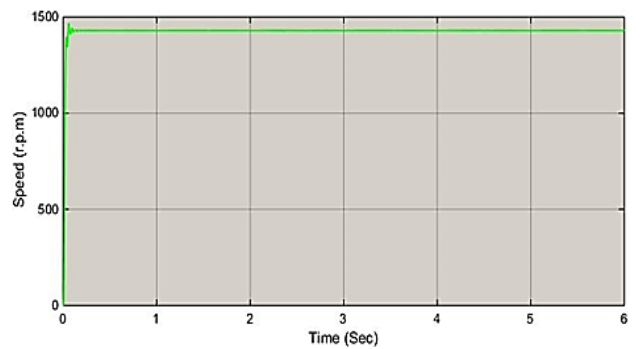


Figure 28b. The rotor speed (r.p.m) for SVPWM based on the carrier frequency at $f_r=50\text{Hz}$.

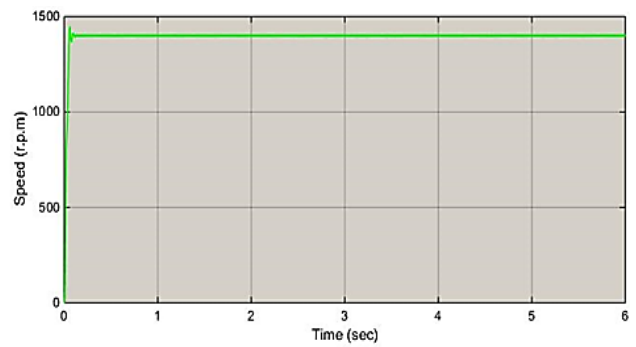


Figure 28c. The rotor speed (r.p.m) for SVPWM based on the carrier frequency with reduced switching at $f_r=50\text{Hz}$.

TABLE II. TOTAL HARMONIC DISTORTION FOR THREE TYPES OF SVPWM

Modulation Types	THD voltage (%)	No- load	Load
		THD current (%)	THD current (%)
M ₁	99.61	8.66	7.19
M ₂	68.42	20.35	12.46
M ₃	85.03	16.15	13.50

TABLE III. PERFORMANCE OF THREE TYPES OF SVPWM INVERTER IN VARIABLE FREQUENCY DRIVE SYSTEM

Status No	f _r (Hz)	M ₁	M ₂	M ₃	M ₁	M ₂	M ₃
		Speed (r.p.m)			Line voltage (V)		
1	10	295	296	296	186	205	205
2	15	434	442	443	205	251	252
3	20	577	587	586	252	290	286
4	25	718	730	733	288	325	336
5	30	853	873	871	313	355	367
6	35	985	1014	1010	333	393	385
7	40	1113	1155	1154	356	420	418
8	45	1242	1294	1281	380	445	426
9	50	1367	1429	1400	401	469	430

M₁: SVPWM based on the sector selection. M₂: SVPWM based on carrier. M₃: SVPWM based on reduced switching.

TABLE IV. THE SYSTEM PERFORMANCE AT HIGH SPEED APPLICATION WITH MINIMUM ELECTROMAGNETIC TORQUE (T_e=1.5N.M)

Status No	f _r (Hz)	M ₁	M ₂	M ₃	M ₁	M ₂	M ₃
		Speed (r.p.m)			Line voltage (V)		
1	60	1788	1791	1793	401	469	430
2	70	2083	2090	2083			
3	80	2375	2386	2381			
4	90	2665	2684	2674			
5	100	2957	2977	2967			
6	120	3532	3565	3549			
7	140	4098	4147	4124			

In above results the following notices can be recorded, the Total harmonic distortion THD is shown in Table II have excellent value in two cases, In our case of variable frequency, the rotor speed is shown in Table III and Table IV, for three types of SVPWM, it can be seen clearly in the Table III, the constant torque region from state (1 to 9). Which is given a wide range of speed below the rated frequency. The system good performance at high speed application with minimum Electromagnetic torque (T_e=1.5N.M).

IX. CONCLUSION

This paper can be drawn through the following idea's importance of speed control of AC motor which is a main part in industrial processes. The PWM techniques that was studied are very suitable for real time implementation due to their simplicity, robustness and ease of tuning.

The SVPWM technique gives an excellent performance with low Total harmonic distortion THD. The paper proposed the inverter with three types of SVPWM technique. Feeding three phase induction motor with large scale fan as mechanical load. The simulation results in Table II. Show the Total harmonic distortion of

motor current in load and no-load conditions, under load condition is very small and acceptable. The inverter output current in load operation is very close to the sinusoidal wave, Moreover, the inverter with SVPWM technique is giving a better performance at low frequency, the waveform of output current in SVPWM based on sector selection is better than other types it content low THD at load is (7.19%), were acceptable and approved by the user, the oscillation in electromagnetic torque is minimum compares with others methods, the SVPWM based on the high carrier frequency without sector selection is a simple, and easy implementation, this methods contain a fair and acceptable THD. Moreover. The proposed inverter with three type of SVPWM techniques is recommended for application in the variable frequency drive VFD.

APPENDIX A

TABLE A.1. INVERTER SPECIFICATION

Quantity	Value
Power electronic switches	6-IGBT
Snubber resistance	1x10 ⁵
Snubber Capacitance	∞
Internal resistance (Ron)	0.0001Ω
Fall and tail time[Tf Tf]	[1 2]μsec
Forward voltages [Device, Diode]	[0.7 0.3]

TABLE A.2. SPECIFICATION AND PARAMETERS OF THE PROPOSED MOTOR

Quantity	Value
Number of phase	3
Mechanic power	5.4 HP, 4KW
Rated voltage	400 v
Rated frequency	50 HZ
Rotor speed	1430 r.p.m
Number of poles	4
Synchronous speed	1500 r.p.m
Slip speed	0.047
Motor parameters & types of frame	
Reference frame	Stationary
Stator resistance	1.405Ω
Rotor resistance	1.395Ω
Stator inductance	5839 mH
Rotor inductance	5839 mH

REFERENCES

- [1] B. K. Bose, *Modern Power Electronic and AC Drives*, Pearson Education, 2003.
- [2] B. K. Bose, *Power Electronics and Motor Drives Advances and Trends*, Elsevier, 2006.
- [3] M. H. Rashid, *Power Electronics, Circuits, Derives and Applications*, Pearson Education Inc., 2004.
- [4] ABCs Technologies Motors/Drives. (2010). The ABCs (and 1-2-3s) of variable frequency. [Online]. Available: <http://machinedesign.com/motorsdrives/abcs-and-1-2-3s-variable-frequency-drives>
- [5] *Technical Guide - Induction Motors Fed by PWM Inverters*, 2ndw, WEG Equipment's Electrics S.A. International Division, 2008.
- [6] D. B. H. W. Van, H. C. Skudelny, and G. V. Stanke, "Analysis and realization of a pulse width modulator based on voltage space vectors," *IEEE Transactions on Industry Applications*, vol. 24, no. 1, pp. 142-150, 1988.

- [7] Texas Instruments, "Scalar (V/f) control of 3-phase induction motors," Application report SPRABQ, July 8, 2013.
- [8] A. V. Niekerk, "Measurement of induction motor parameters using the Voltech PM6000 power analyser," PhD thesis, Murdoch University, 2014.
- [9] J. W. Jung, "Space vector PWM inverter," Department of Electrical and Computer Engineering, The Ohio State University United States of America, February 2008.
- [10] G. Guo and W. You, "Quality analysis of SVPWM inverter output voltage," in *Proc. IEEE International Conference on Computer Science and Software Engineering*, 2008, pp. 126-129.
- [11] S. Ogasawara, H. Akagi, and A. Nabae, "A novel PWM scheme of voltage source inverters based on space vector theory," *Electrical Engineering*, vol. 74, no. 1, pp. 33-41, 1990.
- [12] S. Manivannan, S. Veerakumar, P. Karuppusamy, and A. Nandhakumar, "Certain investigation in performance of three phase voltage source inverter fed induction motor drive by various pulse width modulation techniques," *International Journal of Engineering Research & Technology*, vol. 3, no. 6, pp. 976-988, June 2014.
- [13] J. H. Seo, C. H. Choi, and D. S. Hyun, "A new simplified space-vector PWM method for three-level inverters," *IEEE Transactions on Power Electronics*, vol. 16, no. 4, pp. 545-550, 2001.
- [14] C. Lin, X. Zhang, and Q. Jiang, "Research on SVPWM inverter output control technology," in *Proc. Fifth International Conference on Measuring Technology and Mechatronics Automation*, Hong Kong, 2013, pp. 927-929.
- [15] Z. Zhang, M. Zhou, M. Xiang, and Y. Liu, "PSCAD/EMTDC based SVPWM inverter simulation," in *Proc. International Conference on Sustainable Power Generation and Supply*, Hangzhou, 2012, pp. 1-5.
- [16] Simulink Getting Started Guide Math Works. [Online]. Available: http://www.MATH_works.com/help/pdf_doc/Simulink/sl_gs.pdf



Ahmed. K. Ali received B.Sc. degree in Electrical Engineering from AL-Mustansiriyah University, Baghdad, Iraq 2012. His research interest power electronics and teleconnection field. Moreover, modelling and simulation of power factor correction devices, distribution system, power quality, and renewable energy resources. He also has experience in, information technology and network security.



Ergun Ercelebi received B.S. degree in Electrical and Electronics Engineering from METU, Gaziantep, Turkey in 1990 and M.S. and Ph.D. degrees in Electrical and Electronics Engineering from Gaziantep University in 1992 and 1999 respectively. He was the head of Computer Engineering, University of Gaziantep between 2003 and 2004. He is presently Professor and head of Dept. of Electrical Electronics Department, University of Gaziantep. His research interests include speech processing, image processing, adaptive filters, neural networks, and statistical signal processing wavelet.